1521-0111/12/8204-645–657$25.00
MOLECULAR PHARMACOLOGY
Vol. 82, No. 4
79897/3794027

Mol Pharmacol 82:645–657, 2012

Discovery of Regulators of Receptor Internalization with High-Throughput Flow Cytometry

Yang Wu, Phillip H. Tapia, Gregory W. Fisher, Peter C. Simons, J. Jacob Strouse, Terry Foutz, Alan S. Waggoner, Jonathan Jarvik, and Larry A. Sklar

Department of Pathology (Y.W., L.A.S.) and Center for Molecular Discovery (Y.W., P.H.T., P.C.S., J.J.S., T.F., L.A.S.), School of Medicine, University of New Mexico, Albuquerque, New Mexico; Department of Biological Science (A.S.W, J.J.) and Technology Center of Networks and Pathways (G.W.F., A.S.W., J.J.), Carnegie Mellon University, Pittsburgh, Pennsylvania

Received May 8, 2012; accepted July 5, 2012

ABSTRACT

We developed a platform combining fluorogen-activating protein (FAP) technology with high-throughput flow cytometry to detect real-time protein trafficking to and from the plasma membrane in living cells. The hybrid platform facilitates drug discovery for trafficking receptors such as G protein-coupled receptors and was validated with the β_2-adrenergic receptor (β_2AR) system. When a chemical library containing ~1200 off-patent drugs was screened against cells expressing FAP-tagged β_2ARs, all 33 known β_2AR-active ligands in the library were successfully identified, together with a number of compounds that might regulate receptor internalization in a nontraditional manner. Results indicated that the platform identified ligands of target proteins regardless of the associated signaling pathway; therefore, this approach presents opportunities to search for biased receptor modulators and is suitable for screening of multiplexed targets for improved efficiency. The results revealed that ligands may be biased with respect to the rate or duration of receptor internalization and that receptor internalization may be independent of activation of the mitogen-activated protein kinase pathway.

Introduction

G protein-coupled receptors (GPCRs) constitute the largest protein family in the human genome. They represent the most important class of drug targets (Lefkowitz, 2007). Nearly 30% of all drugs approved by the Food and Drug Administration, including 19 of the top 50 drugs sold in the United States, target GPCRs (Overington et al., 2006; Schlyer and Horuk, 2006). However, current drugs target just ~10% of the 357 nonolfactory GPCRs. Of those that are not current drug targets, ~100 are orphan receptors for which no endogenous ligand is known; the remaining almost certainly include therapeutically important targets that have not yet been exploited. Therefore, the search for new ligands for both ligand-identified and orphan GPCRs is of considerable importance.

High-throughput screening (HTS) is often the most efficient first step for identifying leads regarding new ligands or drugs in large libraries of chemical compounds (Gribbon and Sewing, 2005). Traditional HTS methods use automated plate readers for the measurement of absorbance, fluorescence intensity, fluorescence polarization, or luminescence. Technological advances also permit high-content screening (HCS) (Zanella et al., 2010), fluorescent label-independent screening (Fang et al., 2008), and high-throughput flow cytometry (HTFC) (Ramirez et al., 2003). HCS may require up to 4 to 12 min per 384-well plate for a maximum of three colors in single-field scanning (Y. Wu, unpublished observations). Multiplexing remains challenging, however, and multiple-field scanning, which is frequently required, significantly increases the time required for sample scanning and data analysis, which may be one of the reasons why only a

This research was supported by the National Institutes of Health National Institute of Mental Health [Grants 1U54-MH084690-02, 5U54-MH084690-03, 1R03-MH093192]; and the National Institutes of Health National Center for Research Resources [Grant 5U54-RR022241].

Article, publication date, and citation information can be found at http://molpharm.aspetjournals.org.

http://dx.doi.org/10.1124/mol.112.079897.

ABBREVIATIONS: GPCR, G protein-coupled receptor; FAP, fluorogen-activating protein; β_2AR, β_2-adrenergic receptor; αAR, α-adrenergic receptor; MCF, median channel fluorescence; ISO, isoproterenol; HCS, high-content screening; HTS, high-throughput screening; HTFC, high-throughput flow cytometry; PCL, Prestwick Chemical Library; TO1-2p, sulfonated thiazole orange coupled to diethylene glycol diamine; ICI 118,551, 3-(isopropylamino)-1-[(7-methyl-4-indanyl)oxy]butan-2-ol; RV, response value; DHA, dihydroalprenolol; GFP, green fluorescent protein; DMSO, dimethylsulfoxide; HPSM, HEPES-potassium-sodium-magnesium; ALP, alprenolol; PRO, propranolol; LEVON, levonordefrin; ANI, anisomycin; NAF, naftopidil; DOM, domperidone; PIZ, pizotifen; BUC, bucindolol; CAV, carvedilol; CYC, cycloheximide; AC, adenylate cyclase; ERK, extracellular signal-regulated kinase; MAPK, mitogen-activated protein kinase.

few high-throughput primary screens performed by using HCS can be found in the literature (Bickle, 2010). Instrument and reagent limitations, as well as difficulties in the development of mechanistic biological assays, have restricted label-free approaches from becoming mainstream HTS platforms (Möller and Slack, 2010). HTFC, which was introduced and validated by one of our laboratories (Ramirez et al., 2003), has been used primarily in bead-based and suspension cell-based assays, including multiplex assays targeting GPCRs and GPCR-related proteins (Edwards et al., 2007; Roman et al., 2009; Young et al., 2009; Surviladze et al., 2010). The times required for HTFC are consistently in the range of ~10 to 12 min per 384-well plate, with no significant increase in the time needed for data acquisition or analysis when up to six multiplexed targets are used for each sample well (Surviladze et al., 2010).

Common approaches for GPCR screening include direct measurements of fluorescent ligand binding to the receptor or of downstream actions such as cAMP production, calcium mobilization, or transcriptional activation. These approaches usually rely on measurements of subtle changes in signal intensity or second messenger signals that might not result from the activity of the targeted receptor.

An alternative downstream event that indicates receptor activation is receptor internalization. Activity-dependent GPCR internalization typically requires the activity of G protein receptor kinases and the translocation of β-arrestin from the cytoplasm to the plasma membrane after agonist-dependent GPCR activation. Common assays include the luminescence-based enzyme fragment complementation assay (Olson and Eglen, 2007) and the fluorescence-based GFP-β-arrestin cluster assay and β-lactamase reporter gene expression assay (Lee et al., 2006; Korn and Krausz, 2007; Barnea et al., 2008).

Szent-Gyorgyi et al. (2008) described a number of new reporters, termed fluorogen-activating proteins (FAPs), that bind soluble small-molecule fluorogens. The fluorogens are nonfluorescent in solution but acquire strong characteristic fluorescence when bound to FAPs. FAPs have been fused to the N terminus of the human β_2-adrenergic receptor (β_2AR), and the fusion proteins are functionally comparable with their wild-type counterparts, with no apparent interference with ligand-receptor binding (Fisher et al., 2010).

We combined FAP technology with HTFC to develop a platform for direct monitoring of ligand-induced protein translocation in living cells. The high specificity of the FAP-fluorogen detection system ensures that the fluorescence signal is specific for the target protein, whereas the HTFC system guarantees the throughput and multiplexing capability.

The platform was validated with prototypical β_2ARs. We used the platform to screen against the Prestwick Chemical Library (PCL), to identify compounds that deplete cell surface β_2ARs and compounds that stabilize cell surface β_2ARs. "Hit" molecules were confirmed with concentration-response assays followed by secondary assays. Time- and concentration-dependent experiments to investigate the relationships between several functionally selective β_2AR ligands and receptor endocytosis/total receptor expression levels were performed. Several confirmed compounds that affected β_2ARs in a concentration-dependent manner but had no known connection to the β_2AR internalization pathway are under investigation.

Materials and Methods

Materials. The cell membrane-impermeable fluorogen sulfonated thiazole orange coupled to diethylene glycol diamine (TO1-2p) (excitation wavelength, 509 nm; emission wavelength, 530 nm) was synthesized at Carnegie Mellon University, as described earlier (Szent-Gyorgyi et al., 2008). Plasticware and chemicals were obtained from Sigma-Aldrich (St. Louis, MO) unless stated otherwise.

Production of FAP-β_2AR-Expressing Cells. A plasmid expressing the surface-displayed fusion protein of FAP with the extracellular N terminus of the human β_2AR was generated (Szent-Gyorgyi et al., 2008). Functional FAP-β_2AR fusion protein was successfully expressed in NIH3T3 cells as reported (Szent-Gyorgyi et al., 2008; Fisher et al., 2010). A similar retroviral transfection protocol was applied to express FAP-β_2AR stably in the U937 human monocytic cell line. U937 cells are known to exhibit robust internalization of agonist-stimulated GPCRs and are well suited for high-throughput flow cytometric assays, because U937 is a suspension cell line. The human single-chain antibody AM2.2 (the FAP) binds the cell membrane-impermeable fluorogen TO1-2p with high affinity and increases the fluorescence signal for this fluorogen more than 2000-fold (Szent-Gyorgyi et al., 2008).

Cell Culture. AAM2 cells (U937 cells that stably express surface FAP-β_2ARs, with the FAP moiety able to bind to the fluorogen TO1-2p) were maintained at 37°C in sterile, filtered, RPMI 1640 medium containing 10% heat-inactivated fetal bovine serum, 100 units/ml penicillin, 100 μg/ml streptomycin, 10 mM HEPES, pH 7.4, 20 μg/ml ciprofloxacin, and 2 mM L-glutamine, in a water-jacketed incubator with 5% CO_2/95% air (Thermo Fisher Scientific, Waltham, MA), in tissue culture flasks (Greiner Bio-One GmbH, Frickenhausen, Germany) at a maximal cell density of 400,000 cells/ml until the day of harvesting. For reliability purposes, FAP-β_2AR expression in AAM2 cells was checked daily, and cell cultures with more than 30% of the population without detectable receptor expression were excluded from the experiment. Cells were typically counted and concentrated to 1 to 5 × 10^6 cells/ml before experiments.

Flow Cytometric Characterization of AAM2 Cells. For steady-state receptor expression experiments, AAM2 cells were maintained at 37°C in serum-free RPMI 1640 medium in the presence or absence of the β_2AR full agonist isoproterenol (ISO) or a compound of interest for up to 2 h before the addition of TO1-2p; fluorescence intensity was then measured immediately through flow cytometry. For real-time kinetic experiments, AAM2 cells were maintained at 37°C in RPMI 1640 medium in the presence or absence of 20 μM ISO for up to 90 min. The baseline cell autofluorescence was measured through flow cytometry for 30 s before the addition of fluorogen. Light-scatter and fluorescence signals were measured with either a FACScan flow cytometer (BD Biosciences, San Jose, CA) equipped with a 488-nm laser and a 530/30-nm bandpass filter for the FL1 channel or an Accuri C6 flow cytometer (BD Biosciences) equipped with 488-nm and 640-nm lasers and a 530/50-nm bandpass filter for the FL1 channel. Total copies of surface FAP-β_2ARs were determined by comparing the fluorescence signal for the FL1 channel for TO1-2p bound to cells and a set of FITC-conjugated beads (BD Biosciences).

Confocal Microscopic Imaging. Live-cell, confocal, microscopic images were obtained with a Zeiss 510 META inverse microscope (Carl Zeiss Inc., Thornwood, NY) equipped with four lasers (405, 488, 543, and 633 nm) and a 63× water-immersion objective. Resting cells or cells that had been prestimulated with the desired compounds for up to 120 min were added to a Lab-Tek chambered coverglass system (Thermo Fisher Scientific) at 37°C, after which up to 1 μM TO1-2p was added to the cells in the absence or presence of the compound of interest, and the fluorescence signals were measured by using a 530/50-nm bandpass filter.

High-Throughput Screening of Prestwick Chemical Library. Flow cytometric measurements were performed by using the HyperCyt HTFC platform (IntelliCyt Corp., Albuquerque, NM) (Ramirez et al., 2003). The HTFC platform uses a peristaltic pump in combination with an autosampler and a cytometer. The system enables measurements of microplate wells at rates in excess of one endpoint sample well per second. When the system is used in a multiwell format, the sampling probe of the autosampler moves from one well to the next as a peristaltic pump sequentially aspirates sample particle suspensions from each well. Between wells, the continuously running pump draws a bubble of air into the sample line, to generate a series of bubble-separated samples for delivery to the flow cytometer. Data were collected at a sampling rate of 40 samples (~1 μl) per minute. Because of the nature of the described approach, agonist and antagonist screens were performed separately. AAM2 cells were harvested, centrifuged, resuspended in serum-free RPMI 1640 medium at 4×10^6 cells/ml, and stored at 37°C in a humidified cell culture incubator until the time of the experiments.

For the agonist screen, 5 μl of serum-free RPMI 1640 medium or ISO in RPMI 1640 medium, 100 nl of compound at 1 mM, and 3 μl of cells were added to microtiter plates sequentially by using a NanoQuot microplate dispenser (BioTek Instruments, Winooski, VT), a Biomek FX^P laboratory automation workstation (Beckman Coulter Inc., Fullerton, CA) equipped with a pin tool, and the NanoQuot dispenser, respectively. Positive and negative control wells were included in each plate. Cells in negative control wells received only DMSO vehicle, and cells in positive control wells received 20 μM ISO. The assay plates were removed from the deck and incubated for 90 min at 37°C in a humidified cell culture incubator. TO1-2p was added in 3 μl of RPMI 1640 medium, at a final concentration of 150 nM, by the NanoQuot dispenser. The cells were immediately sampled by using a HyperCyt autosampler, and the fluorescence signals for surface β_2ARs were detected with a Cyan ADP flow cytometer (Beckman Coulter Inc.). The concentration of compound in the assay was 12.5 μM during treatment, which was followed by the addition of TO1-2p.

For the antagonist screen, 5 μl of serum-free RPMI 1640 medium or the β_2AR antagonist 3-(isopropylamino)-1-[(7-methyl-4-indanyl)oxy]-butan-2-ol (ICI 118,551) at 10 μM (final concentration) in RPMI 1640 medium, 100 nl of compound at 1 mM, and 3 μl of cells were added to microtiter plates. The plates were removed from the deck and incubated for 30 min at 37°C in a humidified cell culture incubator before the addition of ISO at 1 μM (final concentration) in 3 μl of RPMI 1640 medium. In this screen, cells that received only DMSO and cells that were treated with 10 μM ICI 118,551 followed by 1 μM ISO served as positive controls, and cells that were treated with 1 μM ISO alone served as negative controls. The assay plates were then incubated in the 37°C cell culture incubator for another 60 min. After the addition of TO1-2p at 150 nM (final concentration) in 3 μl of RPMI 1640 medium, the cells were immediately sampled by using a HyperCyt autosampler, and the fluorescence signals for surface β_2ARs were detected with a Cyan ADP flow cytometer. The concentration of compound in the assay was 9 μM during treatment, which was followed by the addition of TO1-2p.

Hit molecules were determined on the basis of the response value (RV), which represents the percentage of surface β_2AR depletion by agonist or preservation by antagonist and can be calculated with the following equation: $RV = [|MCF_{NCntrl} - MCF_{Sample}|/|MCF_{PCntrl} - MCF_{NCntrl}|] \times 100$, where MCF_{NCntrl}, MCF_{Sample}, and MCF_{PCntrl} represent MCF values for negative control, sample, and positive control wells, respectively. Samples with RVs of ≥50 were considered hits. Because of the high level of stability of this assay, the applied cutoff filter exceeded 6 times the S.D. of the control values.

The quality of the screens was evaluated by using Z' values, which are correlated with MCF and S.D. values for both positive and negative control samples. Z' values of ≥0.5 generally indicate that HTS assays are reliable, with a high degree of confidence that hit molecules have biologically relevant activity (Zhang et al., 1999). Concentration-response relationships for hit compounds between 2 ng/ml and 20 μg/ml (range, 27–142 μM), in half-log unit increments, were measured by using a protocol similar to that described above.

Screening data were analyzed by using HyperView software, which was developed by Bruce Edwards and is available from IntelliCyt. This software automatically resolves data clusters and analyzes each bin to determine mean or median channel forward scatter, side scatter, and fluorescence intensity (MCF) and the number of gated events for each well.

Membrane Preparation and Solubilization of β_2AR-GFP. The procedure was published elsewhere (Simons et al., 2003, 2004). U937 cells expressing a β_2AR-enhanced GRP construct (β_2AR-GFP) on their surfaces were centrifuged at 1200 rpm for 5 min and were resuspended in cavitation buffer (10 mM HEPES, 100 mM KCl, 3 mM $NaCl_2$, 3.5 mM $MgCl_2$, with 1× protease inhibitor cocktail 1 containing bovine lung aprotinin, E-64 protease inhibitor, disodium EDTA, and leupeptin; EMD Biosciences, San Diego, CA), at a density of 10^7 cells/ml. The cells were placed in a pressure bomb and were incubated at 450 psi for 20 min with nitrogen, after which the suspension was slowly released into a sample tube. The suspension was centrifuged at 1200 rpm for 5 min to remove unbroken cells and nuclei. The supernatant, which contained suspended membranes, was pelleted twice through centrifugation at 135,000*g* for 30 min at 4°C; the membrane pellet was resuspended in buffer (25 mM HEPES, pH 7.5, 200 mM sucrose), divided into aliquots of 1×10^8 cell equivalents, and stored at −80°C until the day of the experiments.

Seven hundred microliters of 30 mM HEPES, pH 7.5, 100 mM KCl, 20 mM NaCl, 1 mM $MgCl_2$ (HPSM), were added to an aliquot of thawed soluble membranes (typically 1×10^8 cell equivalents), and the mixture was centrifuged at 13,500*g* at 4°C for 15 min to remove sucrose in the supernatant. The membrane pellet was resuspended in 220 μl of HPSM through passage through a 25-gauge syringe 10 times, after which 25 μl of 10% dodecyl maltoside (DOM) and 2.5 μl of 100× protease inhibitor cocktail were added to the membrane. The mixture was kept in a cold room (4–7°C) for 2 h, with mild vortex-mixing. The mixture was centrifuged at 13,500*g* for 20 min to remove insoluble materials. Soluble receptors were used within 8 h after solubilization.

DHA Bead Competitive Binding Assay. DHA beads were prepared as described previously (Simons et al., 2003, 2004). Equal volumes of epoxy-activated Superdex-peptide beads (GE Healthcare, Chalfont St. Giles, Buckinghamshire, UK) and 0.2 M dithiothreitol in 0.2 M $NaHCO_3$ were mixed and incubated at 37°C for 4 h, to create sulfhydryl-activated beads. The beads were washed five times, and 1 ml of water, 40 mg of (−)-alprenolol (ALP), and 10 μl of 10% ammonium persulfate were added to 1 ml of beads. The reaction mixture was flushed for 5 min with a gentle stream of nitrogen, to remove oxygen, and was kept capped under nitrogen for 2 h at 37°C, with constant mixing. The derivatized beads were washed five times each with water, 50% ethanol, ethanol, water, and HPSM, to remove excess ALP, and were stored at 4°C as a 50% slurry in HPSM with 0.02% NaN_3 and 0.01% DOM.

Typically, 10 μl of stock DHA beads were added to 400 μl of HPSM with 0.1% DOM, 0.1% bovine serum albumin, and 0.05% Tween 20 with light vortex-mixing or rocking in the cold room (4–7°C) for 30 to 60 min, to reduce nonspecific binding. The beads were resuspended in 200 μl of HPSM plus 0.1% DOM. A typical 10-μl binding assay contained 2 μl of soluble receptors, 2 μl of DHA beads, 2 μl of test compounds or buffer, and 4 μl of HPSM with 0.1% DOM. The mixture was prepared and incubated for 2 h in a cold room with mild vortex-mixing before measurements of the forward scatter, side scatter, and fluorescence with an Accuri C6 flow cytometer. All experiments were repeated at least three times in duplicate.

Kinetic Measurements of Surface and Total Receptor Levels in Cells. AAM2 cells or β_2AR-GFP cells were harvested, resuspended in serum-free RPMI 1640 medium at ~500,000 cells/ml for 1

or 18 h, and maintained in a 37°C tissue culture incubator until the time of the experiments. Taking into account the initial 1:1 fusion of the β_2AR with GFP or the FAP tag and the transduction of the fused receptor into cells with pseudo-virus particles, we made the simplifying assumptions that the signals for GFP or fluorogen-bound FAP represented intact β_2ARs and only intact FAP-β_2ARs would have access to the non–membrane-permeable version of the fluorogens under our experimental conditions. For measurements of the total amounts of AM2.2-β_2ARs, AAM2 cells were pretreated with 1 μM TO1-2p for 18 h, with the assumption that all surface and internal FAP-β_2ARs would be accessible to TO1-2p because of basal receptor recycling and probe redistribution. The relatively smaller fractional changes in the total β_2AR-GFP signal, in comparison with the FAP-β_2AR signal, suggest a possible contribution of β_2AR-GFP located in nontrafficking compartments.

At the time of the experiments, cells were exposed to selected drugs and were maintained in a 37°C tissue culture incubator. Aliquots of cells were transferred to sample tubes on ice immediately after the addition of drugs and 30, 60, 90, 120, 180, 240, 300, and 360 min after drug treatment. For measurements of total receptor numbers, the fluorescence signals for β_2AR-GFP cells and AAM2 cells that had been pretreated with 1 μM TO1-2p were measured immediately with an Accuri C6 flow cytometer. In the case of surface receptors, AAM2 cells were allowed to cool on ice for at least 15 min before the addition of 1 μM TO1-2p, and flow cytometric measurements were performed 15 min after exposure to TO1-2p.

Results

Observation of Receptor Internalization. AAM2 cells are U937 cells that stably express surface FAP-β_2ARs, with the FAP moiety pointing outward into the medium. The FAP specifically binds the fluorogen thiazole orange and its derivatives to exhibit fluorescence. Confocal microscopic images of living AAM2 cells are shown in Fig. 1. In each case, the receptors were observed by using the membrane-impermeable fluorogen TO1-2p. Immediately after the addition of TO1-2p (Fig. 1a), strong surface fluorescence was observed. When the same cells were treated for 60 min with the receptor agonist ISO and then exposed to TO1-2p (Fig. 1b), very little fluorescence was observed, presumably because the receptors had been internalized and were no longer available to contact the fluorogen at the cell surface. When the cells were exposed to TO1-2p together with ISO for 60 min, fluorescence signal was observed in the interior compartment of the cells (Fig. 1c). These results indicated that TO1-2p bound to the FAP moiety and then was internalized with the activated receptor. The order and timing of the addition of fluorogen and agonist, as shown in Fig. 1, were critical to the experimental design and outcomes. We could detect either surface-displayed FAP-β_2ARs alone or surface plus internalized receptors in a cell with the addition of fluorogen and receptor agonist at appropriate times.

Functional Characterization of Receptor Internalization through Flow Cytometry. Figure 2 presents quantitative data obtained for AAM2 cells through flow cytometry. The kinetics of TO1-2p binding to untreated and activated cells are shown in Fig. 2a. After baseline fluorescence was recorded for 30 s, 150 nM TO1-2p was added to the cells. Fluorescence signals for resting cells appeared almost immediately, with a $\tau_{1/2}$ value of <5 s; $\tau_{1/2}$ represents the time at which half of the FAPs are occupied by TO1-2p. No detectable signal over cell autofluorescence was recorded from wild-type U937 cells, which indicates that the binding between TO1-2p and FAP is highly specific. Little signal was detected from ISO-prestimulated cells, which is consistent with the imaging results (Fig. 1b) and confirms that the majority of the cell surface receptors were internalized as a consequence of ISO stimulation. Equilibrium binding data

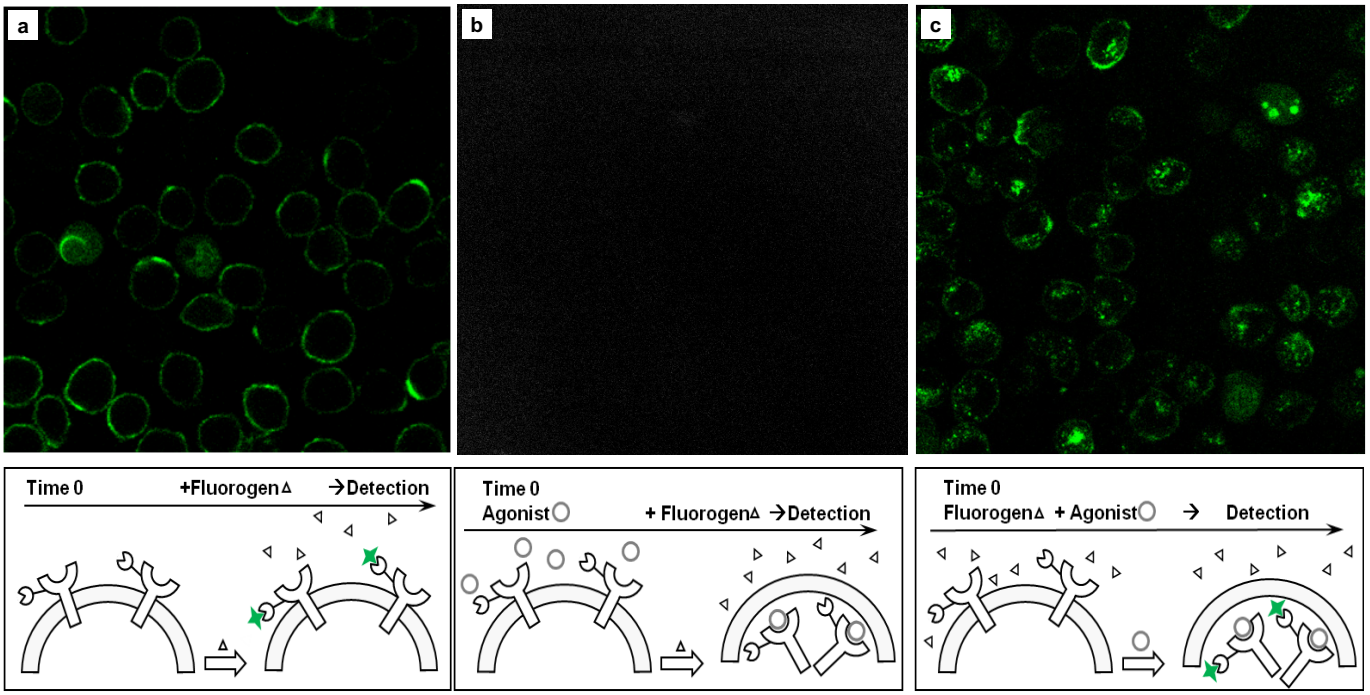

Fig. 1. Internalization of FAP-tagged receptors detected by confocal microscopy. a, image of living AAM2 cells treated with 150 nM TO1-2p, obtained 1 to 60 min after treatment. b, image of living AAM2 cells stimulated with 20 μM ISO for 60 min before the addition of 150 nM TO1-2p, obtained 1 to 15 min after the final addition. c, image of living AAM2 cells treated with 20 μM ISO and 150 nM TO1-2p, obtained 20 to 60 min after the simultaneous additions. Diagrams describe the experimental scheme to acquire each confocal image and the presumed states of the receptor with the FAP tag, fluorogen, and agonist.

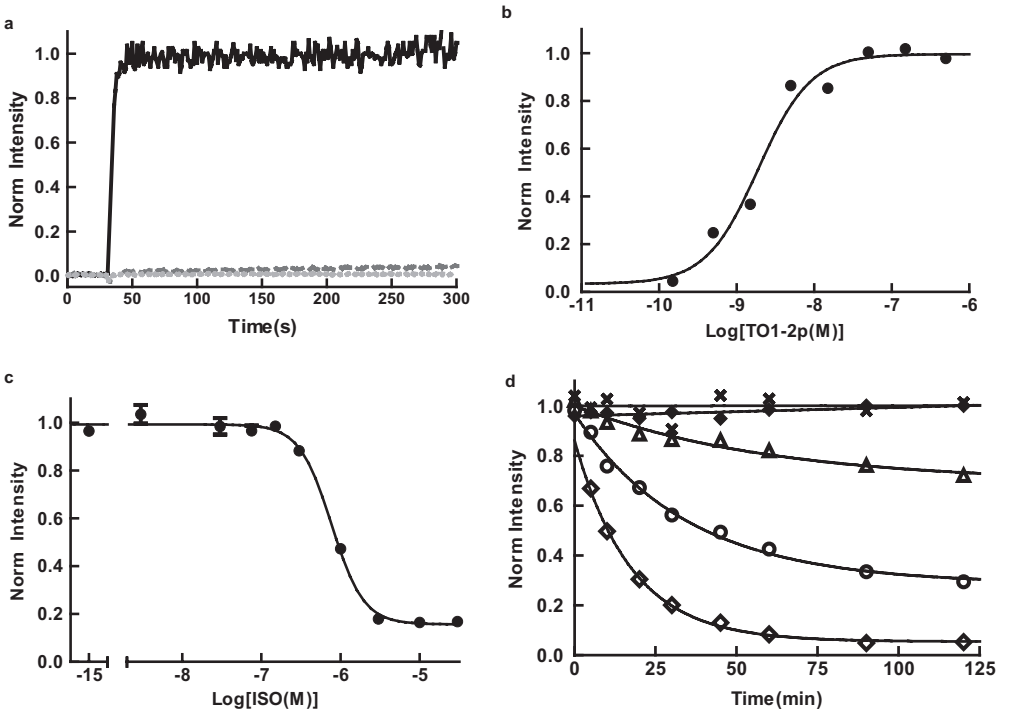

Fig. 2. Flow cytometric characterization of AAM2 cells with TO1-2p, agonist, and antagonist. a and b, kinetic (a) and equilibrium (b) binding of TO1-2p to AAM2 cells. a, binding between TO1-2p and AM2.2 had a half-time of less than 5 s. Solid, dashed, and dotted lines represent the binding of TO1-2p to resting AAM2 cells, ISO-stimulated AAM2 cells, and wild-type U937 cells, respectively. b, TO1-2p binds with high affinity, displaying a K_d value of ~2 nM. c, β_2AR agonist ISO-induced receptor internalization, with an EC_{50} value of ~800 nM. d, time course of surface β_2AR internalization induced by ISO in the absence and presence of the β_2AR antagonist ICI 118,551. Open triangles, open circles, and open diamonds represent the signals for AAM2 cells treated with 0.2, 1, and 20 μM ISO, respectively, solid diamonds represent the signals for resting AAM2 cells, and crosses represent the signals for AAM2 cells treated with 10 μM ICI 118,551 plus 20 μM ISO. Norm, normalized.

for TO1-2p and AAM2 cells showed that the fluorogen bound to FAP-β_2ARs with an affinity of ~2 nM (Fig. 2b), which is consistent with the value for TO1-2p with FAP-β_2ARs expressed in NIH3T3 cells (Szent-Gyorgyi et al., 2008).

The effective concentration for ISO-induced receptor internalization was determined by exposing the cells to ISO for 90 min before the addition of TO1-2p (Fig. 2c). The measured EC_{50} value for receptor internalization was ~0.8 μM, which is comparable with the reported binding affinity between ISO and β_2ARs (Baker et al., 2003a; Hoffmann et al., 2004; Copik et al., 2009).

Receptor antagonists can prevent agonist-induced receptor internalization. The high-affinity β_2AR antagonist ICI 118,551 (Hoffmann et al., 2004) was chosen for this study. Cells were treated with different concentrations of ISO alone or in the presence of 10 μM ICI 118,551 for up to 120 min. ISO alone progressively reduced the number of surface-displayed receptors in a time- and ligand concentration-dependent manner (Fig. 2d). Approximately 15, 60, and 90% of surface-displayed receptors were depleted after 60 min of activation with 0.2, 1, and 20 μM ISO, respectively. The measured half-time of 20 μM ISO-induced FAP-β_2AR internalization was ~11 min. In the presence of 10 μM ICI 118,551, however, even 20 μM ISO had no impact on surface-displayed FAP-β_2ARs. The absolute amount of surface FAP-β_2ARs could be calculated by converting the MCF value to the mean equivalent soluble fluorescence (Supplemental Eq. 1). Results from this series of experiments indicated that the FAP-β_2AR fusion protein and its wild-type counterpart functioned similarly and that TO1-2p exhibited virtually no nonspecific binding to the cells.

HTS of Prestwick Chemical Library. The feasibility and biological reliability of the platform were evaluated through screening against the PCL. The PCL includes 1200 off-patent drugs, 34 of which are known to target β_2ARs, including 10 agonists, 23 antagonists, and a prodrug that was not expected to be an active ligand under our experimental conditions (Tunek and Svensson, 1988). Agonist and antagonist screens were performed separately, because of the differing natures of the approaches, and illustrative results for each are shown (Fig. 3). Cells were treated with 12.5 μM concentrations of each compound for the agonist screen and 9 μM concentrations of each compound for the antagonist screen.

Primary Agonist Screen for FAP-Receptor Internalization. A time-dependent HTFC display for a single 384-well plate is shown in Fig. 3a. For easier viewing, fluorescence results for the first 26 wells are shown in Fig. 3a, inset. Cells from each well of the plate were delivered sequentially to the cytometer, separated by air bubbles that contained no cells. Each colored cluster in the graph represents cells from an individual well of the microtiter plate, the small gaps represent air bubbles between samples, and the large gap toward the end of the graph indicates the end of the row; the last two wells in each row were kept sample-free intentionally. Analyzed data from a single row (row N) are shown in expanded form in Fig. 3b, in which data represent the averaged cell fluorescence values from individual wells. Clear separation between signals for positive control well N1 (12.5 μM ISO) and negative control well N2 (DMSO vehicle) was observed. Signals for most of the sample wells were similar to the negative control signal; however, cells in some wells showed significant decreases in fluorescence, such as the signal for well N11 (Fig. 3b). The compound in that well was the well known β_2AR agonist salmeterol (Keating and McCormack, 2007; Tashkin and Fabbri, 2010). The PCL screen targeting β_2AR agonists was performed twice in duplicate, and the average Z' value for all 16 plates was 0.72.

Hit molecules were determined by using the RV, calculated as described above, which represents the percentage of surface β_2AR depletion. Samples with RVs of ≥50 were considered hits. Because of the high level of stability of this assay,

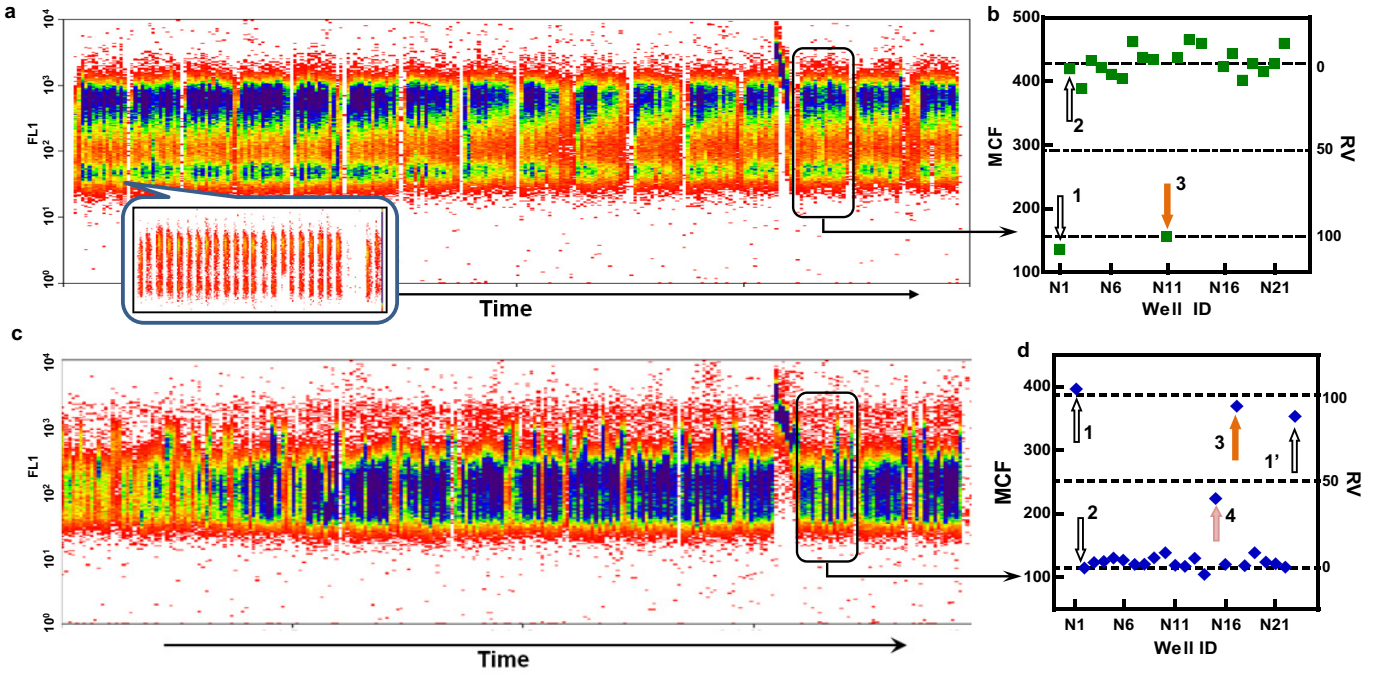

Fig. 3. Screens of a Prestwick Chemical Library plate for FAP-β_2AR ligands yielding internalization (for agonists) or prevention of ISO-induced internalization (for antagonists). a and c, screen shots of time versus fluorescence signals for a complete 384-well plate targeting β_2AR agonists (a) and antagonists (c). Pseudo-color represents the density of cells that emit the same level of fluorescence signal at any given time point; blue represents the highest cell density and red the lowest. Inset, magnified data from the first 26 wells of the plate shown in a. Each cluster represents data from a single well, and the gaps between clusters are air bubbles used to separate the samples. The larger gap toward the end of the trace indicates the end of the row, because the last two wells of each row were intentionally left free of samples. b and d, analyzed data from row N for the screens shown in a and c, respectively. b, point 1, signal for positive control well N1 (12.5 μM ISO); point 2, signal for negative control well N2 (vehicle); point 3, hit for cells treated with a 10 μM concentration of the β_2AR full agonist salmeterol. d, points 1 and 1′, signals for positive control wells N1/N23 (9 μM ICI 118,551 and 1 μM ISO/vehicle); point 2, signal for negative control well N2 (1 μM ISO); point 3, hit for cells treated with a 9 μM concentration of the β_2AR antagonist timolol; point 4, near-hit for cells treated with a 9 μM concentration of the αAR-selective antagonist prazosin.

the applied cutoff filter exceeded 6 times the S.D. of the control values. A total of 23 hits were identified, of which eight were known high-potency agonists for β_2ARs (Table 1). All 23 hits from the primary screen, plus two additional β_2AR agonists and the prodrug (which did not appear among the hits, as expected), were selected for a concentration-response screen for confirmation and potency determination, followed by secondary assays to validate their targets and cellular effects.

Primary Antagonist Screen for Prevention of FAP-Receptor Internalization. The cytometer display for the antagonist screen against the same PCL plate as in Fig. 3a is shown in Fig. 3c, and processed data are shown in Fig. 3d. The separation between signals for positive control wells N1 and N23 (9 μM ICI 118,551 plus 1 μM ISO and vehicle) and negative control well N2 (1 μM ISO) indicated that ICI 118,551 completely inhibited ISO-induced receptor internalization. As in the agonist screen, signals for the majority of wells were similar to those for the negative control wells. Cells in well N17 showed a significant increase in fluorescence, which was attributable to the β_2AR antagonist timolol (Baker, 2005). RV in this assay represents the percentage of stabilized surface β_2ARs, and samples with RVs of >50 were scored as hits. On the basis of this criterion, the elevated fluorescence signal attributable to the compound in well N15 was not scored as a hit (Fig. 3b); the compound was prazosin hydrochloride, an αAR antagonist (Centurión et al., 2006) that displays some cross-reactivity with β-adrenoceptors.

Similar to the agonist screen, the antagonist screen was performed twice in duplicate and yielded an average Z' value of 0.68. A total of 62 hits were identified, including all 23 known β_2AR blockers in the library. Other compounds on the list included some weak β_2AR antagonists and compounds with no known connection with β_2ARs.

High-Throughput Concentration-Response Assays. High-throughput concentration-response assays were performed for all hit compounds, for activity confirmation and potency assignment. Concentration-response curves are shown in Fig. 4 for six representative hit compounds, including agonists (Fig. 4, a–c) and antagonists (Fig. 4, d–f). Hits identified in the primary agonist screen included low-affinity β_2AR ligands such as the β_2AR-selective agonist levonordefrin (LEVON) (Fig. 4a), which induced β_2AR internalization with an expectedly weak EC_{50} of ~50 μM. Some hit molecules with no known connection to β_2ARs, such as the protein synthesis inhibitor anisomycin (ANI) (measured EC_{50}, ~35 nM) (Fig. 4b) and the calcium channel blocker pimozide (Patmore et al., 1989) (measured EC_{50}, ~20 μM) (Fig. 4c), also reduced cell surface expression of β_2ARs in a concentration-dependent manner. Likewise, in the antagonist screen, propafenone (Harron and Brogden, 1987), a class Ic antiarrhythmic medication that has weak β_2AR antagonist activity, prevented ISO-induced β_2AR internalization with an IC_{50} of 0.2 μM (Fig. 4d). Several compounds that have not been reported to be β_2AR ligands, such as naftopidil (NAF) and pizotifen (PIZ), also prevented ISO-induced receptor internalization with submicromolar to micromolar potency (Fig. 4, e and f). Selected results from both screens are sum-

TABLE 1

Comparison of β_2AR ligands in Prestwick Chemical Library

Known agonists, known antagonists, and unusual compounds are included, in that order. The function of each compound reported in the literature (agonist or antagonist) and the affinities measured in competitive radioligand binding assays (reported in the literature), FAP-β_2AR internalization assays, and soluble β_2AR-GFP-DHA bead competitive binding assays are reported.

	Function (Reported)	LogEC$_{50}$/IC$_{50}$			References
		Receptor Internalization		DHA Binding	
		Literature	Measured		
Salbutamol	Agonist	5.8–6.1	5.7 ± 0.3	5.3	Isogaya et al., 1999; Hoffmann et al., 2004; Park, 2005
Fenoterol	Agonist	6.9	6.8 ± 0.1	5.5	January et al., 1997; Hoffmann et al., 2004; Park, 2005
Isoetharine	Agonist		5.7 ± 0.5	5.4	
Salmeterol	Agonist	8.8	>8.5	7.7	January et al., 1998; Hoffmann et al., 2004
(+)-Isoproterenol	Agonist	6.4	5.6 ± 0.3	4	Hoffmann et al., 2004
(−)-Isoproterenol	Agonist	6.4	6.4 ± 0.4	6	Hoffmann et al., 2004
Clenbuterol	Agonist	7.9	7.2 ± 0.2	6.2	Baker, 2010
Terbutaline	Agonist	5.6	5.0 ± 0.5	5.4	Baker, 2005
Metaproterenol	Agonist		5.0 ± 0.1	4.8	
Ritodrine	Agonist	3.5–4.5	>4	4.8 ± 0.2	Baker, 2010
Acebutolol	Antagonist	6.0–6.4	4.8 ± 0.1	3.8	Baker, 2005
Betaxolol	Antagonist	7.2	5.3 ± 0.1	5.1	Smith and Teitler, 1999; Baker, 2005
Pindolol	Antagonist	9–9.4	8.4 ± 0.2	8.7	Baker, 2010
Bisoprolol	Antagonist		5 ± 0.1	4.7	
(*S*)-Atenolol	Antagonist			5.5 ± 0.1	
(*R*)-Atenolol	Antagonist	5.0–6.0	6.4 ± 0.4	6	Smith and Teitler, 1999; Baker, 2005
Nadolol	Antagonist	7.0–8.6	7.7	8.5	Candelore et al., 1999; Baker, 2005
Alprenolol	Antagonist	9	>8.5	8.5 ± 0.3	Hoffmann et al., 2004
(*S*)-Propranolol	Antagonist	9.1–9.5	>8.5	>9	Hoffmann et al., 2004
(*R*)-Propranolol	Antagonist	7.3	6.8 ± 0.1	6.7 ± 0.2	Baker, 2005
(±)-Propranolol, 50/50	Antagonist	9.1–9.5	7.9	8.5 ± 0.2	Smith and Teitler, 1999; Baker et al., 2003b; Baker, 2005
Timolol	Antagonist	9.7	>8.5	>9	Sharif et al., 2001; Baker, 2005
Metoprolol	Antagonist	6.3–6.9	5.5 ± 0.5	5.5 ± 0.3	Smith and Teitler, 1999; Baker, 2005
(+)-Levobunolol	Antagonist		6.85	6.8	
(−)-Levobunolol	Antagonist	9.0–9.9	>8.5	>9	Sharif et al., 2001
Labetalol	Antagonist	8 ± 0.1	7.0	7	Baker, 2005
Oxprenolol	Antagonist	9.0	>8.5	9	Baker, 2010
Penbutolol	Antagonist		>8.5	>9	
Pronethalol	Antagonist		6.2 ± 0.3	5.7	
Sotalol	Antagonist	6.8 ± 0.1	6 ± 0.1	6.25	Baker, 2005
Carteolol	Antagonist		>8.5	>9	
Xamoterol	Antagonist	6.1 ± 0.1	4.6 ± 0.1	4.8	Baker, 2005
Practolol	Antagonist	7.1 ± 0.1	N.A.	N.A.	Baker, 2005
Bambuterol	Prodrug	N.A.			N.A.
Levonordefrin[a]	Weak agonist		4.4 ± 0.4	4.3 ± 0.1	N.A.
Propafenone[b]	Weak antagonist		6.7	7.4 ± 0.1	
Anisomycin[a]	N.A.		7.3 ± 0.3	<3	
Naftopidil[b]	N.A.		6.7 ± 0.2	4.5 ± 0.5	
Domperidone[b]	N.A.		5.5 ± 0.5	<3	
Pizotifen[b]	N.A.		5 ± 0.1	<3	
Maprotiline[a]	N.A.		4.1 ± 0.1	6.7	
Boldine[b]	N.A.		4.1 ± 0.2	5.9	

N.A., not applicable.
[a] Hit in agonist screen.
[b] Hit in antagonist screen.

marized in Table 1. Two secondary assays, that is, a competitive binding assay and confocal microscopy, were used to validate the hits identified in the primary screens.

β_2AR-DHA Competitive Binding Assay. This assay was based on the direct binding of solubilized β_2AR-GFP, a fusion protein of β_2AR and enhanced green fluorescent protein, to beads derivatized with DHA (Simons et al., 2003). The fluorescence measured was from bead-bound β_2AR-GFP. When a β_2AR agonist or antagonist competes with ALP (the presumed ligand structure after the linkage of DHA to the beads) for binding to the receptor, a decrease in bead fluorescence is expected (Fig. 5a). Concentration-response curves for several agonists and antagonists are shown in Fig. 5, b and c. The EC$_{50}$/IC$_{50}$ values, or potencies, for β_2AR hits from the primary PCL screens that were measured with this bead-based assay were typically in close agreement with the measured potencies for receptor internalization (agonists) or for prevention of internalization (antagonists), as well as with literature-reported K_d values for β_2AR binding affinities. Summary data for all 33 known β_2AR ligands identified as hits in the primary screen, plus the prodrug bambuterol and eight of the "unexpected" hits, are shown in Table 1.

Most of the compounds identified through the primary screens and concentration-response confirmation assays were found to induce β_2AR internalization (or to prevent ISO-induced β_2AR internalization) and to couple to β_2ARs with similar EC$_{50}$ values. For some compounds, significantly different potencies (>100-fold differences) were measured with the two assays. Among these compounds were ANI (identified in the agonist screen) and NAF, DOM, and PIZ

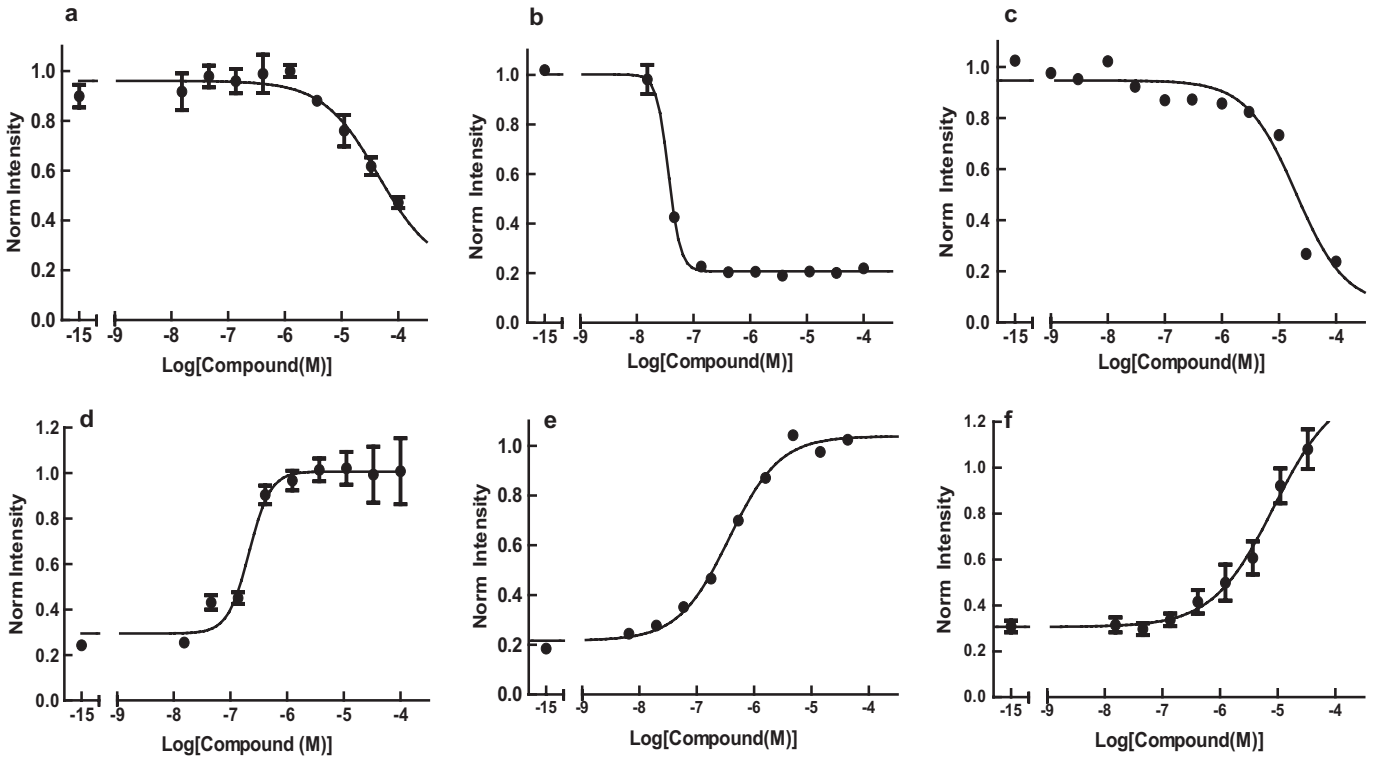

Fig. 4. Concentration-response curves for FAP-receptor internalization or stabilization with selected hit compounds from the PCL agonist screen (a–c) and antagonist screen (d–f). a, levonordefrin, an αAR agonist (EC_{50} = 4.5 × 10^{-5} M). b, anisomycin (EC_{50} = 3.5 × 10^{-8} M). c, pimozide (EC_{50} = 2 × 10^{-5} M). d, propafenone (IC_{50} = 2.1 × 10^{-7} M). e, naftopidil (IC_{50} = 1.2 × 10^{-7} M). f, pizotifen (IC_{50} = 8.6 × 10^{-6} M). Norm, normalized.

(identified in the antagonist screen). These compounds all induced receptor internalization (or prevented ISO-induced internalization) at significantly lower concentrations than the concentrations at which they competed with bead-borne DHA for binding to the receptor. The situation was reversed for maprotiline (agonist) and boldine (antagonist). The conflicting results suggest that these compounds do not compete with the same binding site on β_2ARs as does ALP but might be noncanonical regulators of β_2ARs, compounds that induce receptor internalization in a receptor-biased manner, or compounds that nonspecifically decrease surface receptor expression.

Live-Cell Confocal Microscopic Imaging of AAM2 and β_2AR-GFP-Transfected Cells. To investigate further the compounds that showed apparent inconsistencies in affinities measured with the two different methods, we monitored the behavior of both FAP-β_2AR cells and β_2AR-GFP cells in response to these compounds by using confocal microscopy. For AAM2 cells, TO1-2p at a saturating concentration was added to the cells together with the compounds.

Fluorescence micrographs were obtained for untreated FAP-β_2AR and β_2AR-GFP cells (Fig. 6, a and g), cells stimulated with 20 μM ISO (Fig. 6, b and h), cells exposed to both 10 μM ALP and 1 μM ISO (Fig. 6, e and k), and cells incubated with 10 μM concentrations of the active molecules ANI (Fig. 6, c and i), LEVON (Fig. 6, d and j), and NAF plus 1 μM ISO (Fig. 6, f and l). Although ANI was identified as active in the β_2AR agonist concentration-response assay, with an

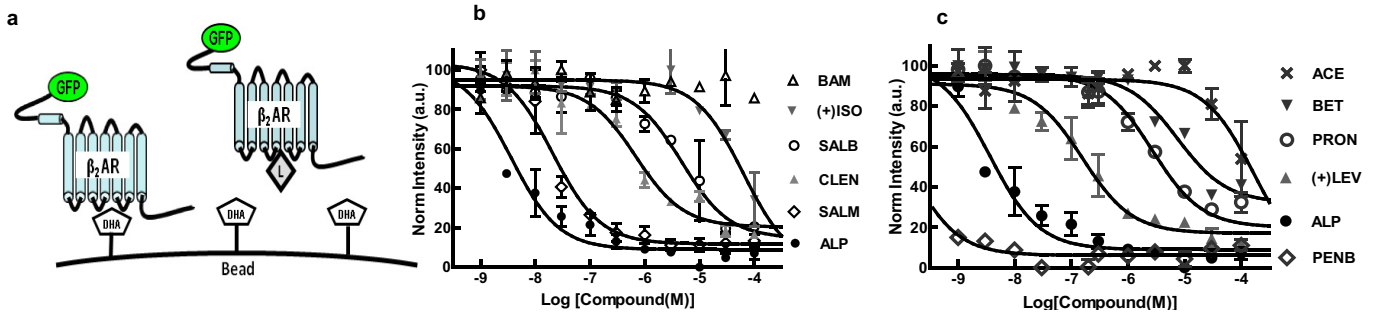

Fig. 5. β_2AR-GFP-DHA bead competitive binding assay. a, schematic diagram of the HTFC-compatible β_2AR-DHA competitive binding assay. Soluble β_2AR-GFP can bind to dihydroalprenolol-derivatized beads at high affinity (left receptor), whereas β_2AR ligands (agonists or antagonists) can block the binding between the receptor and the beads (right receptor), leading to decreased fluorescence signals for the beads. b, concentration-response curves for selected agonists measured with the β_2AR-DHA competitive binding assay. The *y*-axis indicates normalized (Norm) bead fluorescence intensity, in arbitrary units (a.u.). c, concentration-response curves for selected antagonists measured with the β_2AR-DHA competitive binding assay. ALP served as the positive control for the experiment. All experiments were performed in duplicate at least three times. EC_{50} values for all β_2AR ligands and several active compounds can be found in Table 1. BAM, bambuterol; SALB, salbutamol; CLEN, clenbuterol; SALM, salmeterol; ACE, acebutolol; BET, betaxolol; PRON, pronethalol; (+)LEV, (+)-levobunolol; PENB, penbutolol.

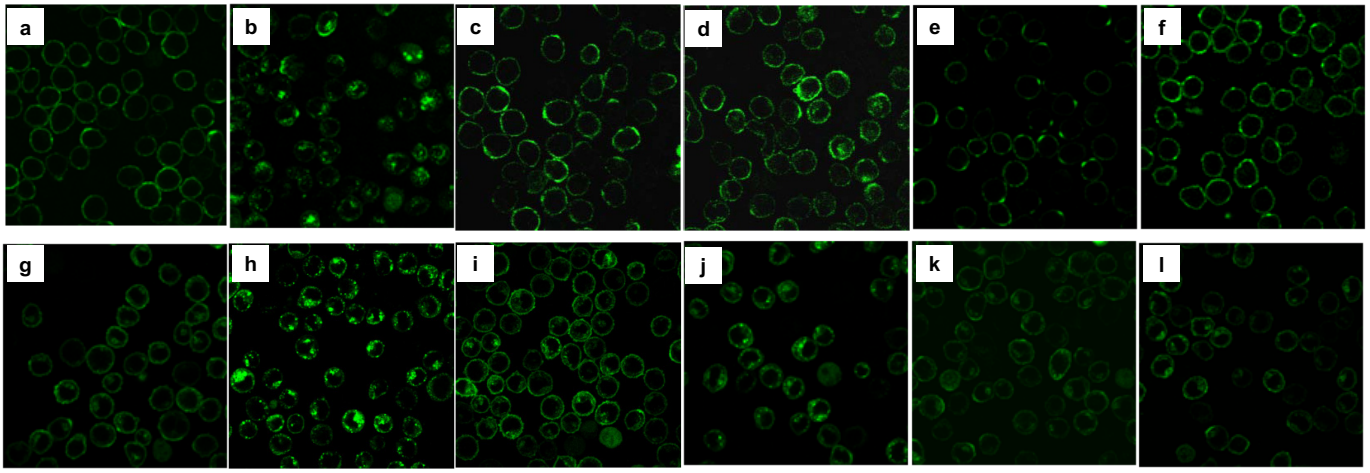

Fig. 6. Confocal microscopic images of AAM2 cells (a–f) and β_2AR-GFP cells (g–l) obtained in parallel, demonstrating the extent of receptor internalization. For AAM2 cells, a saturating concentration of TO1-2p was added to the cells together with the compounds, to track the translocation of FAP-β_2ARs. a and g, untreated cells of both cell types showed receptors largely on the plasma membrane, with little receptor internalization. b and h, cells of both cell types that were treated for 1 h with a 10 μM concentration of the β_2AR agonist ISO showed more receptors internalized than on the surface (high receptor internalization levels). c and i, test cells that were treated with 10 μM anisomycin showed little internalization, which classified these compounds as nonagonists of receptor internalization. e and k, cells that were treated with the β_2AR antagonist ALP plus 1 μM ISO showed little internalization. d and j, cells that were treated with 10 μM LEVON showed a certain degree of receptor internalization, indicating that LEVON acts as a weak agonist of β_2AR. f and l, test cells that were treated with 10 μM naftopidil plus 1 μM ISO also showed little internalization, which classified this compound as an antagonist of receptor internalization.

EC_{50} of ~35 nM, 10 μM ANI did not induce β_2AR internalization in either of the cell lines (Fig. 6, c and i), in contrast to the β_2AR agonist ISO (Fig. 6, b and h) and the active compound LEVON (Fig. 6, d and j). For ANI, the loss of surface fluorescence when cells were preincubated with the compound and then treated with fluorogen resulted not from the expected internalization but through some other mechanism. Hit molecules identified in the antagonist screen that were not known β_2AR antagonists, including NAF (Fig. 6, f and l), DOM, boldine, and PIZ (Supplemental Fig. 1), all prevented ISO-induced β_2AR internalization in both cell lines, although significant capping seemed to occur. Taken together with the β_2AR-DHA competition binding assay results, the validation approaches facilitated the identification of compounds that induced β_2AR internalization through noncanonical pathways from compounds that nonspecifically decreased the expression of receptors.

Drug Effects on Surface and Total β_2AR Levels in Cells over Time. Figure 7 shows the amounts of surface and total AM2.2-β_2AR and the total amounts of β_2AR-GFP over 6 h in the presence or absence of selected drugs. For convenience, the average MCF value at time 0 was normalized to 1. As shown in Fig. 7a, the total amount of β_2AR-GFP in untreated cells was nearly stable over the course of the experiment. The β_2AR-GFP levels appeared to increase slightly for cells treated with both ISO and LEVON, whereas the protein synthesis inhibitor cycloheximide (CYC) gradually reduced total receptor expression in the cells, as expected. Six hours after exposure to CYC, approximately 80% of the β_2ARs remained. The results obtained with ANI were completely different from those obtained with the other drugs. The compound reduced the surface AM2.2-β_2AR level to the same level as observed with ISO within 2 h after treatment and maintained the lower level. In contrast, the

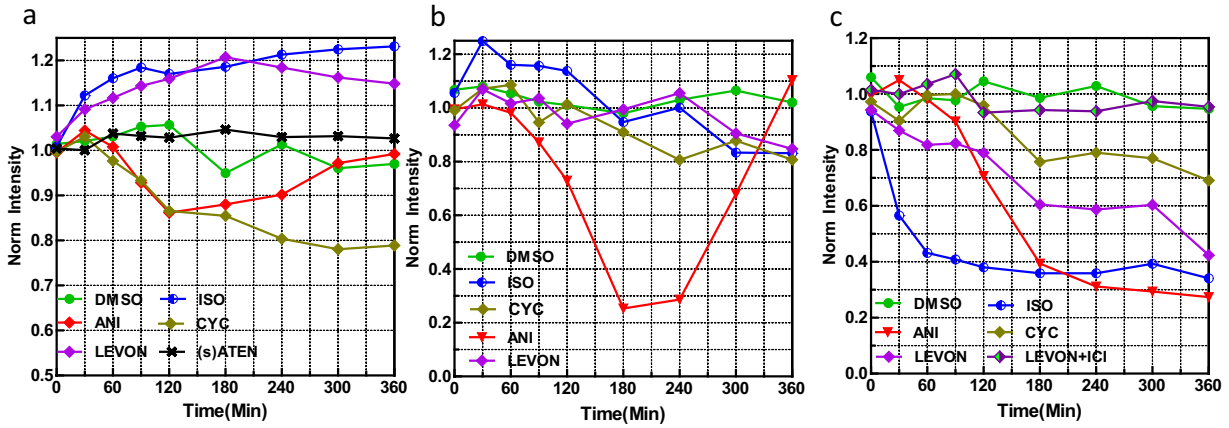

Fig. 7. Time course of changes in cell surface and total β_2AR levels. Cell total and surface receptor levels were measured 0, 30, 60, 90, 120, 180, 240, 300, and 360 min after drug treatment. a, untreated β_2AR-GFP cells (DMSO) and cells treated with 10 μM ISO, 10 μM ANI, 10 μM CYC, 10 μM LEVON, or 10 μM (s) Atenolol (ATEN) together with 1 μM ISO. b, AAM2 cells preincubated with 1 μM TO1-2p before drug treatment and analysis. c, untreated AAM2 cells and cells treated with 10 μM ISO, 10 μM ANI, 10 μM CYC, or 10 μM LEVON. An aliquot of cells was removed from the stock and cooled on ice for 15 min. TO1-2p (1 μM) was added to the cells and the mixture was incubated for 15 min before flow cytometric measurements. Norm, normalized.

total receptor levels in both AAM2 and β_2AR-GFP cells were decreased for the first 2 to 3 h and then returned to the same level as in untreated cells. This behavior was observed in five separate experiments.

Similar experiments were performed with functionally selective β_2AR ligands, including bucindolol (BUC), carvedilol (CAV), propranolol (PRO), and atenolol, and results were compared with those obtained with the β_2AR agonist ISO, which activates both adenylate cyclase (AC) and extracellular signal-regulated kinase (ERK) 1/2 pathways (Galandrin and Bouvier, 2006). We monitored total and surface receptor levels in the presence and absence of these drugs for up to 6 h. This set of experiments helped define the relationships between the activation of ligand-induced GPCR downstream pathways and receptor endocytosis. As shown in Fig. 8, none of the compounds tested reduced surface receptor levels alone at up to 1 μM concentrations within 5 h after the addition of the compound. In contrast, BUC, CAV, and PRO prevented ISO-induced β_2AR internalization with IC_{50} values of 1.8, 1.5, and 0.7 nM, respectively. The IC_{50} values were close to literature values for the binding affinities of these ligands for β_2ARs (Pauwels et al., 1988; Pönicke et al., 2002; Hoffmann et al., 2004).

Discussion

Although GPCRs are the molecular targets of nearly 30% of all drugs approved by the Food and Drug Administration, most members of the GPCR superfamily have not been explored as drug targets and their contributions to drug side effects have not been systematically investigated. Therefore, the search for new ligands for ligand-identified and orphan GPCRs is of considerable importance. These ligands might include classic receptor agonists and antagonists as well as noncanonical, functionally selective ligands, the discovery of which might be the starting point for the design of new therapeutic agents (Shenoy et al., 2006), including those that differentially activate a subset of receptor functions or induce internalization without activation, thereby optimizing therapeutic benefits while minimizing side effects (Mailman, 2007; Kenakin, 2011).

We have described a powerful platform for GPCR screening that combines FAP technology with high-throughput flow cytometry and that was shown to detect and to quantify β_2AR responses; we think that this platform provides a unique opportunity to discover new drug leads regardless of their molecular properties. Our protocol was optimized for screens against human β_2ARs with consistent results, and it was used to identify compounds that induced β_2AR internalization and those that antagonized β_2AR internalization. The molecules identified in the pilot screens included all of the active β_2AR ligands in the test library when a cutoff filter that exceeded 3 times the S.D. of the control signal was used. Bambuterol, an inactive prodrug of the β_2AR agonist terbutaline that requires a hydrolytic and/or oxidative reaction to produce the active compound, was not identified, as expected (Tunek and Svensson, 1988). At least 20 weak regulators of β_2ARs with EC_{50}/IC_{50} values greater than 1 μM were also identified. The potencies of compounds measured with receptor internalization assays and soluble receptor competitive binding assays and reported ligand-receptor binding affinities were similar for the most part (Table 1), which suggests that this approach correctly identifies orthosteric receptor ligands.

By following the developed HTS protocols, the activities of compounds that regulated surface β_2AR internalization with potencies above 100 μM were validated in secondary assays. The bead-based β_2AR-DHA competitive binding assay allowed us to distinguish direct interactions between β_2ARs and their canonical ligands (such as ISO) from more-complex GPCR signaling pathways. This HTS-compatible assay was used as the first approach to confirm findings for ligands competing for the same binding site as ALP. It is noteworthy that this assay could be used to distinguish compounds that induced receptor internalization through noncanonical pathways but was insensitive to compounds that reduced surface receptor levels in an alternative or nonselective way (e.g., protein synthesis inhibitors). Live-cell microscopic analysis was used to record receptor trafficking in real time and to provide visual confirmation of the receptor locations.

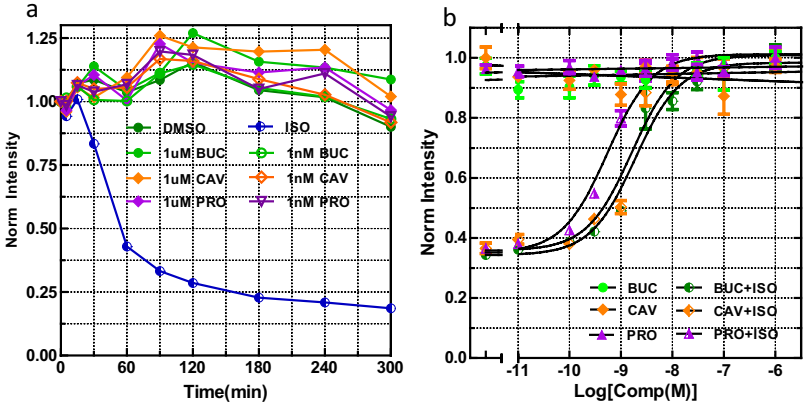

Fig. 8. a, time course comparison of cell surface AM2.2-β_2AR levels in the presence of 1% DMSO, 1 μM ISO, 1 μM BUC, 1 nM BUC, 1 μM CAV, 1 nM CAV, 1 μM (*S*)-PRO, or 1 nM (*S*)-PRO. Cell surface receptor levels were measured 0, 30, 60, 90, 120, 180, 240, and 300 min after drug treatment. ISO (10 μM) progressively induced receptor internalization, and DMSO had no effect on surface receptor expression. All other compounds tested did not induce receptor internalization up to 5 h after treatment. b, concentration-response curves for FAP receptor stabilization with BUC, CAV, or (*S*)-PRO in the presence of 1 μM ISO. The presence of up to 1 μM BUC, CAV, or (*S*)-PRO alone did not induce any surface receptor internalization, and all three compounds effectively prevented ISO-induced receptor internalization, with nanomolar efficacy [BUC, IC_{50} = 1.8 nM; CAV, IC_{50} = 1.5 nM; (*S*)-PRO, IC_{50} = 0.7 nM]. Norm, normalized.

We cross-validated both assays by testing the compounds identified in the high-throughput concentration-response assays. Observations from these two assays demonstrated the potential for efficient removal of certain classes of false-positive compounds at this early stage of drug discovery and validation of changes in the cellular distribution of receptors. During this investigation of hit molecules from the original PCL screen, we found several new ligands for β_2ARs, including LEVON, an αAR agonist that behaved in a manner very similar to that of the β_2AR agonist ISO (Fig. 7; Table 2).

The identification of unexpected compounds indicates that our approach does not rely on the binding of compounds to any specific binding site of the receptor or require receptor internalization through any specific pathway; therefore, it allows a search for noncanonical receptor modulators. For instance, the "false-agonist" ANI decreased the amounts of surface-displayed FAP-β_2ARs without inducing receptor internalization, which indicates that the receptor internalization assay can identify compounds that reduce the number of surface receptors regardless of the mechanism of action. ANI, which was originally thought to be a protein synthesis inhibitor, appeared to function differently from the protein synthesis inhibitor CYC. Unlike CYC, which consistently down-regulated total β_2AR-GFP and AM2.2-β_2AR levels over time, ANI gradually reduced total β_2AR levels during the first few hours after exposure but levels unexpectedly recovered to basal levels thereafter. Surface receptor levels remained low during the same period. Taken together with results from the DHA bead binding assay, these observations suggest that ANI is neither a canonical β_2AR ligand nor a protein synthesis inhibitor. The identification of this compound proves that the platform described is capable of searching for compounds that induce surface protein endocytosis through any mechanism, and it suggests the promising contribution of the platform to the search for noncanonical receptor regulators, which would be of pharmaceutical significance because of their potential for reduced side effects.

The FAP technology makes it possible to understand the connection between GPCR-related downstream pathways and receptor internalization. After ligand activation, β_2ARs couple to Gα_s or Gα_i proteins and subsequently regulate both AC and mitogen-activated protein kinase (MAPK) pathways. Although most ligands have balanced efficacies for the two pathways, many are reported to have different efficacies (Kenakin, 2002; Azzi et al., 2003; Seifert and Dove, 2009; Vilardaga et al., 2009; Evans et al., 2010). Table 2 compares the efficacy patterns of selected PCL compounds for AC and ERK1/2 (a subfamily of MAPK) pathways, as well as total and surface receptor levels and the ability to induce surface receptor internalization.

Known β_2AR ligands in Table 2 belong to four categories: 1) agonist for both AC and ERK1/2 pathways (ISO), 2) agonist for the ERK1/2 pathway and inverse agonist for the AC pathway (PRO), 3) agonist for the ERK1/2 pathway and neutral ligand for the AC pathway (BUC and CAV), and 4) inverse agonist for both AC and ERK1/2 pathways (atenolol) (Galandrin and Bouvier, 2006). Results showed that ISO and the hit molecule LEVON were the only compounds that yielded elevated total receptor levels with decreased surface receptor levels attributable to ligand-induced receptor internalization. These results indicate that the mechanism of action of LEVON is similar to that of ISO, as an orthosteric β_2AR full agonist. Although it is thought that vesicle-mediated endocytosis is required for activation of the GPCR-related MAPK pathway (Daaka et al., 1998), none of the other agonists of the ERK1/2 pathway had any effect on total or surface receptor levels or induced receptor internalization during the first 6 h after drug treatment. All three compounds reported as β_2AR antagonists and ERK1/2 agonists in the literature (PRO, BUC, and CAR) effectively blocked ISO-induced internalization with nanomolar IC_{50} values.

The platform can be readily extended to other GPCRs, other families of surface receptors (such as receptor tyrosine kinases), or any signaling receptors involving an endocytic or exocytic process (Sorkin and von Zastrow, 2009). The reported agonist assay has already been adapted to screen the National Institutes of Health Molecular Libraries Small Molecule Repository, which contains 340,000 compounds; data from this screen were reported in PubChem (PubChem BioAssay identifier nos. 504448, 504454, and 504459) and will be discussed elsewhere. The combination of FAP with HTFC clearly can take advantage of the sensitivity of fluorogens and FAP binding and the quantitative aspects of flow cytometric assays with high throughput capabilities, which allowed us to complete the Molecular Libraries Small Molecule Repository screen in 8 days. In theory, the FAP assay could be performed with well-based tissue culture plates. However, the relative speed, cost, and quantitative aspects of the high-resolution screen or HCS must be considered. Because flow cytometry is more widespread (tens of thousands of units throughout the world) than high-content analysis (hundreds

TABLE 2

Comparison of efficacy patterns of selected β_2AR ligands and PCL hits for AC and ERK1/2 pathways, effects on total and surface receptor levels, and abilities to induce surface receptor internalization

Compound	Pathway[a]		Effects on Receptor Levels		Receptor Internalization
	AC	ERK1/2	Total	Surface	
(*S*)-Atenolol	INV	INV	No change	No change	INV
Bucindolol	NEUT	AGO	No change	No change	INV[b]
Carvedilol	NEUT	AGO	No change	No change	INV[c]
Propranolol	INV	AGO	No change	No change	INV
Isoproterenol	AGO	AGO	Increase	Decrease	AGO
Cycloheximide	N.A.	N.A.	Decrease	Decrease	N.A.
Anisomycin	N.A.	N.A.	Decrease then increase	Decrease	N.A.
Levonordefrin	N.A.	N.A.	Increase	Decrease	AGO

INV, inverse agonist; NEUT, neutral antagonist; AGO, partial or full agonist; N.A., not applicable.

[a] Galandrin and Bouvier (2006).

[b] Measured IC_{50} = 2.0 ± 0.3 nM (inhibition of ISO-induced internalization).

[c] Measured $IC_{50} \approx$ 1.5 nM (inhibition of ISO-induced internalization).

of units) and the entry cost for a sample-handling system is relatively low, we suggest that flow cytometry might be a popular counterpart or alternative to HCS.

It is now apparent that membrane trafficking is a highly complex but essential signaling process in which 1) multiple receptors in a single cell can signal in response to a single stimulus and 2) a single receptor can trigger multiple downstream effectors through different mechanisms, depending on the ligand. The discoveries of biased agonists, native ligands that induce receptor ubiquitination and down-regulation, and compounds that induce differential sorting pathways all indicate the potential value of GPCR trafficking assays as tools in the field of drug discovery (Jean-Alphonse and Hanyaloglu, 2011). The development of the FAP-based high-throughput flow cytometry platform provides a unique opportunity for researchers in this area.

This platform also has the potential to increase the efficiency of screens through multiplexing. Through fusion of different FAP tags that bind to fluorogens with different emission wavelengths, signals for different receptors expressed in the same cells can be detected simultaneously, with no increase in unwanted background fluorescence. This might be an attractive approach for study of the behavior of a receptor/coreceptor pair upon ligand activation, such as the receptor/coreceptor pair CD4/CXCR4 for HIV entry, $\alpha_v\beta_3$/decay-accelerating factor for Sin Nombre virus entry, or GPCR-induced epidermal growth factor receptor activation, which has been connected to many different types of cancer. Variations in fluorogens and FAPs for pulse-chase experiments also are expected to be available soon.

Acknowledgments

We thank Dr. Tione Buranda for valuable discussion of the manuscript and the University of New Mexico Cancer Center Shared Microscopy Resource.

Authorship Contributions

Participated in research design: Wu, Waggoner, Jarvik, and Sklar.

Conducted experiments: Wu, Tapia, Simons, and Foutz.

Contributed new reagents or analytic tools: Fisher, Strouse, and Jarvik.

Performed data analysis: Wu.

Wrote or contributed to the writing of the manuscript: Wu, Simons, Jarvik, and Sklar.

References

Azzi M, Charest PG, Angers S, Rousseau G, Kohout T, Bouvier M, and Piñeyro G (2003) β-Arrestin-mediated activation of MAPK by inverse agonists reveals distinct active conformations for G protein-coupled receptors. *Proc Natl Acad Sci USA* **100:**11406–11411.

Baker JG (2005) The selectivity of β-adrenoceptor antagonists at the human β1, β2 and β3 adrenoceptors. *Br J Pharmacol* **144:**317–322.

Baker JG (2010) The selectivity of β-adrenoceptor agonists at human β_1-, β_2- and β_3-adrenoceptors. *Br J Pharmacol* **160:**1048–1061.

Baker JG, Hall IP, and Hill SJ (2003a) Agonist and inverse agonist actions of β-blockers at the human β_2-adrenoceptor provide evidence for agonist-directed signaling. *Mol Pharmacol* **64:**1357–1369.

Baker JG, Hall IP, and Hill SJ (2003b) Influence of agonist efficacy and receptor phosphorylation on antagonist affinity measurements: differences between second messenger and reporter gene responses. *Mol Pharmacol* **64:**679–688.

Barnea G, Strapps W, Herrada G, Berman Y, Ong J, Kloss B, Axel R, and Lee KJ (2008) The genetic design of signaling cascades to record receptor activation. *Proc Natl Acad Sci USA* **105:**64–69.

Bickle M (2010) The beautiful cell: high-content screening in drug discovery. *Anal Bioanal Chem* **398:**219–226.

Candelore MR, Deng L, Tota L, Guan XM, Amend A, Liu Y, Newbold R, Cascieri MA, and Weber AE (1999) Potent and selective human β_3-adrenergic receptor antagonists. *J Pharmacol Exp Ther* **290:**649–655.

Centurión D, Mehotra S, Sánchez-López A, Gupta S, MaassenVanDenBrink A, and Villalón CM (2006) Potential vascular α1-adrenoceptor blocking properties of an array of 5-HT receptor ligands in the rat. *Eur J Pharmacol* **535:**234–242.

Copik AJ, Ma C, Kosaka A, Sahdeo S, Trane A, Ho H, Dietrich PS, Yu H, Ford AP, Button D, et al. (2009) Facilitatory interplay in α_{1a} and β_2 adrenoceptor function reveals a non-G_q signaling mode: implications for diversification of intracellular signal transduction. *Mol Pharmacol* **75:**713–728.

Daaka Y, Luttrell LM, Ahn S, Della Rocca GJ, Ferguson SSG, Caron MG, and Lefkowitz RJ (1998) Essential role for G protein-coupled receptor endocytosis in the activation of mitogen-activated protein kinase. *J Biol Chem* **273:**685–688.

Edwards BS, Young SM, Saunders MJ, Bologa C, Oprea TI, Ye RD, Prossnitz ER, Graves SW, and Sklar LA (2007) High-throughput flow cytometry for drug discovery. *Expert Opin Drug Discov* **2:**685–696.

Evans BA, Sato M, Sarwar M, Hutchinson DS, and Summers RJ (2010) Ligand-directed signalling at β-adrenoceptors. *Br J Pharmacol* **159:**1022–1038.

Fang Y, Frutos AG, and Verklereen R (2008) Label-free cell-based assays for GPCR screening. *Comb Chem High Throughput Screen* **11:**357–369.

Fisher GW, Adler SA, Fuhrman MH, Waggoner AS, Bruchez MP, and Jarvik JW (2010) Detection and quantification of β_2AR internalization in living cells using FAP-based biosensor technology. *J Biomol Screen* **15:**703–709.

Galandrin S and Bouvier M (2006) Distinct signaling profiles of β_1 and β_2 adrenergic receptor ligands toward adenylyl cyclase and mitogen-activated protein kinase reveals the pluridimensionality of efficacy. *Mol Pharmacol* **70:**1575–1584.

Gribbon P and Sewing A (2005) High-throughput drug discovery: what can we expect from HTS? *Drug Discov Today* **10:**17–22.

Harron DW and Brogden RN (1987) Propafenone: a review of its pharmacodynamic and pharmacokinetic properties, and therapeutic use in the treatment of arrhythmias. *Drugs* **34:**617–647.

Hoffmann C, Leitz MR, Oberdorf-Maass S, Lohse MJ, and Klotz KN (2004) Comparative pharmacology of human beta-adrenergic receptor subtypes - characterization of stably transfected receptors in CHO cells. *Naunyn Schmiedebergs Arch Pharmacol* **369:**151–159.

Isogaya M, Sugimoto Y, Tanimura R, Tanaka R, Kikkawa H, Nagao T, and Kurose H (1999) Binding pockets of the β_1- and β_2-adrenergic receptors for subtype-selective agonists. *Mol Pharmacol* **56:**875–885.

January B, Seibold A, Allal C, Whaley BS, Knoll BJ, Moore RH, Dickey BF, Barber R, and Clark RB (1998) Salmeterol-induced desensitization, internalization and phosphorylation of the human β_2-adrenoceptor. *Br J Pharmacol* **123:**701–711.

January B, Seibold A, Whaley B, Hipkin RW, Lin D, Schonbrunn A, Barber R, and Clark RB (1997) β_2-Adrenergic receptor desensitization, internalization, and phosphorylation in response to full and partial agonists. *J Biol Chem* **272:**23871–23879.

Jean-Alphonse F and Hanyaloglu AC (2011) Regulation of GPCR signal networks via membrane trafficking. *Mol Cell Endocrinol* **331:**205–214.

Keating GM and McCormack PL (2007) Salmeterol/fluticasone propionate: a review of its use in the treatment of chronic obstructive pulmonary disease. *Drugs* **67:**2383–2405.

Kenakin T (2002) Efficacy at G-protein-coupled receptors. *Nat Rev Drug Discov* **1:**103–110.

Kenakin T (2011) Functional selectivity and biased receptor signaling. *J Pharmacol Exp Ther* **336:**296–302.

Korn K and Krausz E (2007) Cell-based high-content screening of small-molecule libraries. *Curr Opin Chem Biol* **11:**503–510.

Lee S, Howell B, and Kunapuli P (2006) Cell imaging assays for G protein-coupled receptor internalization: application to high-throughput screening. *Methods Enzymol* **414:**79–98.

Lefkowitz RJ (2007) Seven transmembrane receptors: something old, something new. *Acta Physiol (Oxf)* **190:**9–19.

Mailman RB (2007) GPCR functional selectivity has therapeutic impact. *Trends Pharmacol Sci* **28:**390–396.

Möller C and Slack M (2010) Impact of new technologies for cellular screening along the drug value chain. *Drug Discov Today* **15:**384–390.

Olson KR and Eglen RM (2007) β Galactosidase complementation: a cell-based luminescent assay platform for drug discovery. *Assay Drug Dev Technol* **5:**137–144.

Overington JP, Al-Lazikani B, and Hopkins AL (2006) How many drug targets are there? *Nat Rev Drug Discov* **5:**993–996.

Park JB (2005) *N*-Coumaroyldopamine and *N*-caffeoyldopamine increase cAMP via beta 2-adrenoceptors in myelocytic U937 cells. *FASEB J* **19:**497–502.

Patmore L, Duncan GP, and Spedding M (1989) Interaction of palmitoyl carnitine with calcium antagonists in myocytes. *Br J Pharmacol* **97:**443–450.

Pauwels PJ, Gommeren W, Van Lommen G, Janssen PAJ, and Leysen JE (1988) The receptor binding profile of the new antihypertensive agent nebivolol and its stereoisomers compared with various beta-adrenergic blockers. *Mol Pharmacol* **34:**843–851.

Pönicke K, Heinroth-Hoffmann I, and Brodde OE (2002) Differential effects of bucindolol and carvedilol on noradenaline-induced hypertrophic response in ventricular cardiomyocytes of adult rats. *J Pharmacol Exp Ther* **301:**71–76.

Ramirez S, Aiken CT, Andrzejewski B, Sklar LA, and Edwards BS (2003) High-throughput flow cytometry: validation in microvolume bioassays. *Cytometry A* **53:**55–65.

Roman DL, Ota S, and Neubig RR (2009) Polyplexed flow cytometry protein interaction assay: a novel high-throughput screening paradigm for RGS protein inhibitors. *J Biomol Screen* **14:**610–619.

Schlyer S and Horuk R (2006) I want a new drug: G-protein-coupled receptors in drug development. *Drug Discov Today* **11:**481–493.

Seifert R and Dove S (2009) Functional selectivity of GPCR ligand stereoisomers: new pharmacological opportunities. *Mol Pharmacol* **75:**13–18.

Sharif NA, Xu SX, Crider JY, McLaughlin M, and Davis TL (2001) Levobetaxolol (Betaxon) and other beta-adrenergic antagonists: preclinical pharmacology, IOP-lowering activity and sites of action in human eyes. *J Ocul Pharmacol Ther* **17:**305–317.

Shenoy SK, Drake MT, Nelson CD, Houtz DA, Xiao K, Madabushi S, Reiter E, Premont RT, Lichtarge O, and Lefkowitz RJ (2006) β-Arrestin-dependent, G protein-independent ERK1/2 activation by the β_2 adrenergic receptor. *J Biol Chem* **281:**1261–1273.
Simons PC, Biggs SM, Waller A, Foutz T, Cimino DF, Guo Q, Neubig RR, Tang WJ, Prossnitz ER, and Sklar LA (2004) Real-time analysis of ternary complex on particles: direct evidence for partial agonism at the agonist-receptor-G protein complex assembly step of signal transduction. *J Biol Chem* **279:**13514–13521.
Simons PC, Shi M, Foutz T, Cimino DF, Lewis J, Buranda T, Lim WK, Neubig RR, McIntire WE, Garrison J, et al. (2003) Ligand-receptor-G-protein molecular assemblies on beads for mechanistic studies and screening by flow cytometry. *Mol Pharmacol* **64:**1227–1238.
Smith C and Teitler M (1999) Beta-blocker selectivity at cloned human $beta_1$- and $beta_2$-adrenergic receptors. *Cardiovasc Drugs Ther* **13:**123–126.
Sorkin A and von Zastrow M (2009) Endocytosis and signalling: intertwining molecular networks. *Nat Rev Mol Cell Biol* **10:**609–622.
Surviladze Z, Waller A, Wu Y, Romero E, Edwards BS, Wandinger-Ness A, and Sklar LA (2010) Identification of a small GTPase inhibitor using a high-throughput flow cytometry bead-based multiplex assay. *J Biomol Screen* **15:**10–20.
Szent-Gyorgyi C, Schmidt BF, Schmidt BA, Creeger Y, Fisher GW, Zakel KL, Adler S, Fitzpatrick JA, Woolford CA, Yan Q, et al. (2008) Fluorogen-activating single-chain antibodies for imaging cell surface proteins. *Nat Biotechnol* **26:**235–240.
Tashkin DP and Fabbri LM (2010) Long-acting beta-agonists in the management of chronic obstructive pulmonary disease: current and future agents. *Respir Res* **11:**149.
Tunek A and Svensson LA (1988) Bambuterol, a carbamate ester prodrug of terbutaline, as inhibitor of cholinesterases in human blood. *Drug Metab Dispos* **16:**759–764.
Vilardaga JP, Bünemann M, Feinstein TN, Lambert N, Nikolaev VO, Engelhardt S, Lohse MJ, and Hoffmann C (2009) GPCR and G proteins: drug efficacy and activation in live cells. *Mol Endocrinol* **23:**590–599.
Young SM, Bologa CM, Fara D, Bryant BK, Strouse JJ, Arterburn JB, Ye RD, Oprea TI, Prossnitz ER, Sklar LA, et al. (2009) Duplex high-throughput flow cytometry screen identifies two novel formylpeptide receptor family probes. *Cytometry A* **75:**253–263.
Zanella F, Lorens JB, and Link W (2010) High content screening: seeing is believing. *Trends Biotechnol* **28:**237–245.
Zhang JH, Chung TD, and Oldenburg KR (1999) A simple statistical parameter for use in evaluation and validation of high throughput screening assays. *J Biomol Screen* **4:**67–73.

Address correspondence to: Yang Wu, Department of Pathology, School of Medicine, University of New Mexico, MSC08 4640, 700 Camino de Salud NE, IDTC Rm 2340, Albuquerque, NM 87131. E-mail: yawu@salud.unm.edu